Cryogenically-cooled periodically-poled lithium niobate wafer stacks for multi-cycle terahertz pulses

P. J. Dalton,[1, 2, a)] C. T. Shaw,[1, 2, a)] J. T. Bradbury,[1, 2] C. D. W. Mosley,[1, 2] A. Sharma,[3] V. Gupta,[3] J. Bohus,[3] A. Gupta,[3] J.-G. Son,[3] J. A. Fülöp,[3] R. B. Appleby,[1, 2] G. Burt,[1, 4] S. P. Jamison,[1, 5] M. T. Hibberd,[1, 2] and D. M. Graham[1, 2]

[1)]*The Cockcroft Institute, Sci-Tech Daresbury, Keckwick Lane, Daresbury, Warrington WA4 4AD, United Kingdom*

[2)]*Department of Physics and Astronomy & Photon Science Institute, The University of Manchester, Oxford Road, Manchester M13 9PL, United Kingdom*

[3)]*ELI-ALPS Research Institute, ELI-HU Non-Profit Ltd., 6728 Szeged, Hungary*

[4)]*School of Engineering, Lancaster University, Bailrigg, Lancaster LA1 4YW, United Kingdom*

[5)]*Department of Physics, Lancaster University, Bailrigg, Lancaster LA1 4YB, United Kingdom*

(*Electronic mail: patrick.dalton@postgrad.manchester.ac.uk)

(Dated: 5 September 2024)

We report on the generation of high-power narrow-bandwidth terahertz (THz) pulses by cryogenic cooling of hand-made periodically-poled lithium niobate (PPLN) wafer stacks. As a proof-of-concept, we cool stacks with up to 48 wafers down to 97 K and achieve few-percent bandwidths at a center frequency of 0.39 THz, with pulse energy up to 0.42 mJ and average power of 21 mW. Supported by modelling, we observe effective cooling of PPLN wafer stacks that not only reduces THz absorption but critically maintains the micron-scale inter-wafer gaps for optimal THz transmission. Our results unlock the potential for scaling these large-area sources to greater numbers of wafers to push both the energy and bandwidth beyond current capability, opening up possibilities in areas such as THz-driven particle acceleration, THz imaging, and control over material properties.

[a)]These two authors contributed equally

There is a need to develop laser-generated sources of high-energy narrowband terahertz (THz) radiation for application in a broad range of research areas including selective excitation of resonant modes in materials,[1] non-linear microscopy[2] and compact particle accelerators[3]. Recent progress in producing such a source has been based on stacking lithium niobate wafers to mimic periodically-poled bulk crystals, achieved through rotating the ferroelectric z-axis of each consective wafer by 180°. The technique introduced by Lemery *et al.*[4] offers the advantage of constructing large-area sources by exploiting the well-established commercial manufacture of optical-quality wafers. To date, these hand-made periodically-poled lithium niobate (PPLN) wafer stacks, constructed from 50 mm diameter wafers, have demonstrated 1.3 mJ THz pulses at a frequency of 0.16 THz when pumped by a Joule-class laser (a conversion efficiency of 0.14%)[4] and THz conversion efficiencies up to 0.17% at a frequency of 0.39 THz[5]. To increase the THz output further and achieve narrower bandwidths requires increasing the number of wafers in the stack beyond the 12 used by Lemery *et al.*[4] and the 20 used by Mosley *et al.*[5]. However increasing the total thickness of lithium niobate is a challenge due to the large material absorption at THz frequencies resulting in the re-absorption of the generated THz radiation as it propagates through the wafer stack.

It is well-known that cryogenic cooling of lithium niobate can reduce the large material absorption at THz frequencies, due to low-frequency phonon modes,[6] and increase the THz output power.[7–9] It is also known that cryogenic cooling of bulk PPLN crystals can reduce the bandwidth of the THz emission.[10] Lee *et al.*[10] were able to suppress the strong temporal decay of the THz waveform, due to THz absorption, which was observed at room temperature and obtain an 18 GHz bandwidth at 1.8 THz. Carbajo *et al.*[11] reported a fivefold increase in extracted THz energy when cooling a PPLN crystal that emitted at a frequency of 0.52-0.56 THz from 295 K to 100 K. Furthermore, a THz pulse with an energy of 0.458 mJ at 0.36 THz has been reported from the cryogenic cooling of a custom 10×15 mm^2 PPLN crystal to less than 100 K,[12], but a chirped-pulse-beating scheme was required to reduce the laser intensity below the damage threshold due to the bulk crystal aperture limitations.

While wafer stacks offer the advantage of scaling to large area and laser pump spot sizes, the key difference in comparison to bulk crystals is the existence of small inter-wafer gaps on the order of the total thickness variation (TTV) specification of the wafers (typically on the order of 10 µm). These air gaps have been shown to act as THz Fabry-Pérot etalons[5], where increasing gap size reduces THz transmission between wafers and adds a phase-shift which can alter the PPLN

phase matching condition and the generated THz frequency. Whether hand-made PPLN wafer stacks can benefit similarly from cryogenic cooling, and what role thermal expansion plays on the inter-wafer gaps, remain open questions.

In this Letter, we explore cryogenic cooling of hand-made PPLN wafer stacks to <100 K for high-energy narrowband THz generation. The multi-cycle waveforms were directly measured using electro-optic sampling and shown to maintain a flat-top electric field profile for stacks up to 48 wafers when cooled to 97 K. A comparison to a 1-dimensional model of THz generation in PPLN wafer stacks revealed that both the inter-wafer gaps and the THz absorption are sufficiently small at a temperature of <100 K not to have a significant detrimental effect on the emission, and that these sources have significant potential for further increasing the output THz pulse energy and reducing the bandwidth.

The lithium niobate wafers used in this experiment were 5 mol.% magnesium oxide-doped, congruent, *x*-cut, with a diameter of 50.8 mm, a nominal thickness of 135 µm, and had a TTV of less than 10 µm. They were anti-reflection coated on both sides for 1030 nm +/- 60 nm. The wafer thickness corresponded to a poling period of 270 µm, and a THz output frequency around 0.4 THz in the forward propagation direction. The wafer stacks were assembled by hand and placed between two uncoated optical windows; a 6 mm thick CaF_2 window at the entrance and a 12 mm thick ultraviolet fused silica (UVFS) window at the exit of the stack. The two windows provided uniform compression to the wafer stacks, while the UVFS window at the exit acted to minimise the Fresnel loss and maximise THz extraction.

The experiment was carried out using the THz pump laser system at the ELI-ALPS research facility in Szeged, Hungary.[13] The system consists of a fiber oscillator, a fiber stretcher, a regenerative amplifier, several thin disk multipass amplifiers and a grating compressor. It was capable of outputting 500 mJ pulses at a repetition rate of 50 Hz, with a central wavelength of 1030 nm, and a pulse duration compressible down to 500 fs. The experimental setup is shown schematically in Figure 1. The laser output was split into a pump and probe beam, with the pump polarized along the *z*-axis of the wafers. A maximum excitation fluence of 216 mJ cm^{-2} was obtained by focusing the pump beam using a dielectic focusing mirror with a 3 m focal length. The focal point had to be positioned after the PPLN wafer stack in order to limit the fluence and prevent damage caused by structure in the pump beam profile; recorded using a laser beam profiler.

The PPLN wafer stack assembly was mounted on the cold finger of an ultra-low vibration closed-cycle cryostat (K100 CryoCooler, Cryospectra) using spring loaded clips. The cryostat

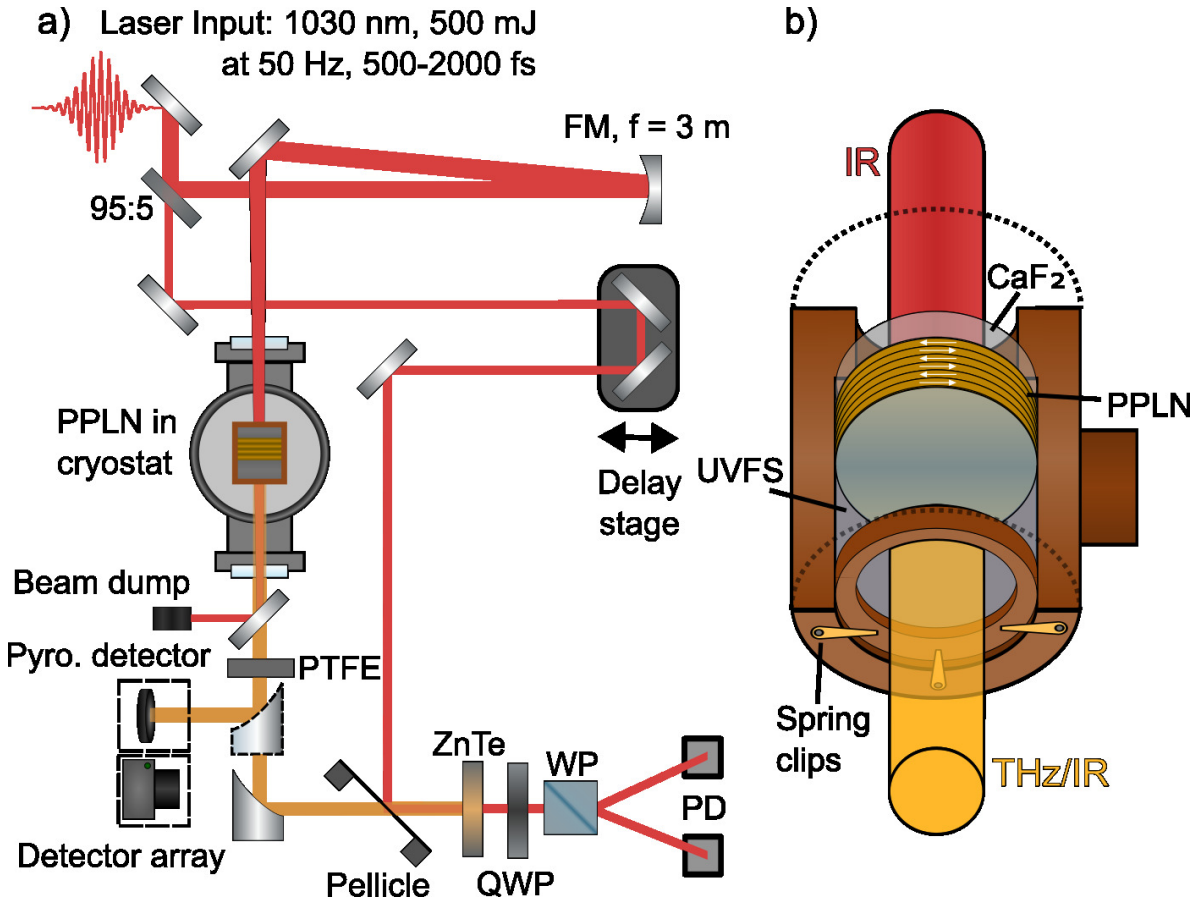

FIG. 1. (a) Schematic diagram of the experimental setup for THz generation and detection. (b) Cutaway drawing of the oxygen-free copper mount that holds the PPLN wafer stack assembly on the cryostat cold finger. QWP = quarter waveplate, WP = Wollaston prism, PD = photodiodes, FM = focusing mirror.

was fitted with a 3 mm thick CaF_2 entrance window (anti-reflection coated for 750-1550 nm), a 6 mm thick CaF_2 or MgF_2 exit window, evacuated to 10^{-6} mbar, and cooled to a base temperature of 97 K. At the exit of the cryostat a 45° high-reflecting 1030 nm dielectric mirror was used to direct the laser pump beam into a beam dump, with a polytetrafluoroethylene (PTFE) plate used to block any residual laser light. The transmitted THz radiation was then focused using either a gold coated 4-inch focal length 90° off-axis parabolic mirror onto a pyroelectric detector (THz-30, Sensor und Lasertechnik GmbH) or an uncooled microbolometric detector array (Microxcam-384i, INO), or by using a gold coated 6-inch focal length 90° off-axis parabolic mirror onto a (110)-cut 4 mm thick ZnTe crystal for electro-optic detection using a boxcar integrator (GIA100, Artifex Engineering GmbH) with an integration time of approximately 10 µs. The pyroelectric detector was connected to a voltage preamplifier and was supplied with a calibration from PTB

Berlin (the German National Metrological Institute).

Figure 2 shows the THz waveforms recorded at room temperature (RT) for the PPLN wafer stacks built up from 10, 30 and 48 wafers. All waveforms were recorded using a positively chirped laser pulse duration of 1.2 ps, as Mosley *et al.*[5] had previously found this close to the optimum conversion efficiency. The waveforms reveal two distinct frequency components corresponding to

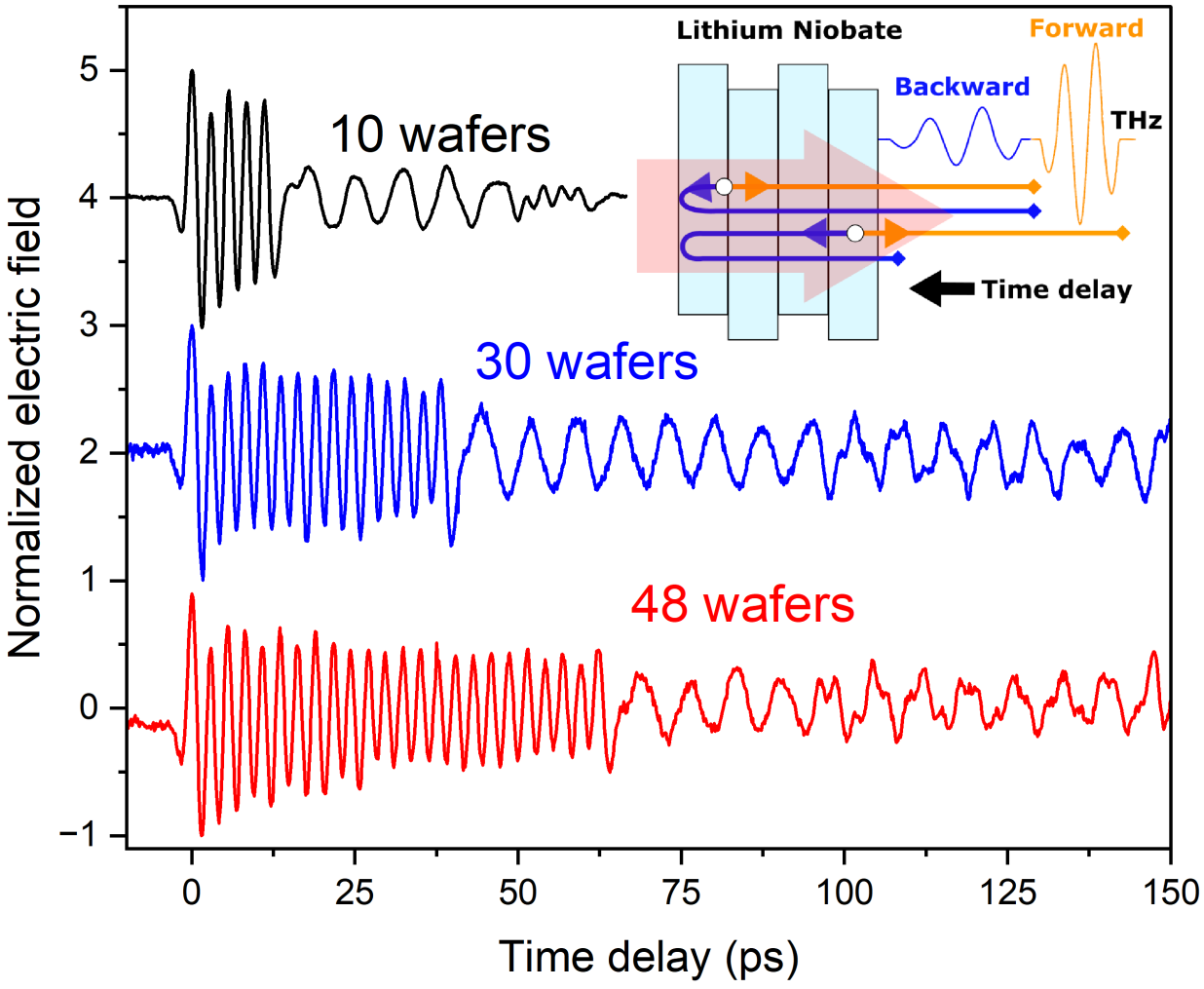

FIG. 2. Normalized THz waveforms recorded for PPLN wafer stacks consisting of 10, 30 and 48 wafers at room temperature using an excitation fluence of 50 mJ cm^{-2} and a positively chirped pulse duration of 1.2 ps. Note, for the 10 wafer PPLN stack a higher excitation fluence of 111 mJ cm^{-2} was used. The waveforms are vertically offset for clarity. Inset shows a schematic diagram depicting the origin of the forward and backward THz generation within the PPLN wafer stack and its relationship with the measured THz waveforms.

0.14 THz and 0.37 THz (see supplementary material for power spectrum). The higher frequency 0.37 THz component starts at a time delay of 0 ps and originates from the forward generated THz pulse exiting from the last wafer within the stack (see inset of Figure 2). The lower frequency 0.14 THz component starts at the end of the high frequency waveform (at approximately 14, 42 and 66 ps for the PPLN wafer assemblies with 10, 30 and 48 wafers, respectively). The 0.14 THz component is due to the backward generated THz pulse which is reflected into the forward direction at the lithium niobate/CaF_2 interface at the entrance of the wafer stack and exits at the same time as the forward generated THz from the first wafer in the stack. The windows sandwiching the PPLN wafer stack, the cryostat exit window and the ZnTe electro-optic crystal thickness were all carefully chosen to move all the reflections outside of the time delay range of the 0.37 THz frequency part of the waveforms in order to prevent distortions. For the 0.37 THz waveform generated using 48 wafers the peak-to-peak amplitude of the last cycle of the waveform decreases to 40% of amplitude of the first cycle.

To explore the impact of cryogenic cooling on a PPLN wafer stack, the 48 wafer stack was subsequently cooled to approximately 97 K, and the THz waveforms remeasured over the time delay range of the 0.37 THz component. Figure 3 a) shows the THz waveform measured at room temperature and two waveforms recorded at 97 K, the first two using a positively chirped pulse duration of 1.2 ps and the third a positively chirped pulse duration of 0.6 ps. The longer duration pulse was used in the majority of the experiments out of caution to avoid optical damage, with a limited number of shorter pulse duration experiments carried out at the end of the ELI-ALPS user time. As can be seen, the decay in amplitude of the waveform is reduced as the temperature decreases. The difference in the amplitude of this decay between the two 97 K waveforms (labelled II and III in Fig. 3) is attributed to the first cold measurement (II) being performed before the PPLN wafer stack had reached thermal equilibrium. This is also evident from the corresponding power spectra in Figure 3 b), where a lower THz emission frequency (0.390 THz) was measured in comparison to the second waveform measured at 97 K (0.394 THz). When the PPLN wafer stack had reached thermal equilibrium (labelled III in Fig. 3), the peak-to-peak amplitude of the last cycle of the waveform remained at 78% of the amplitude of the first cycle, highlighting a significant reduction of the THz absorption/loss at low temperature.

Figures 3 a) and b) show the results of fitting the experimentally measured THz waveforms with a one-dimensional model of THz generation in PPLN wafer stacks. The model considers optical rectification in the PPLN wafer stacks using the wave equation in the crystal with a χ^2 non-linear

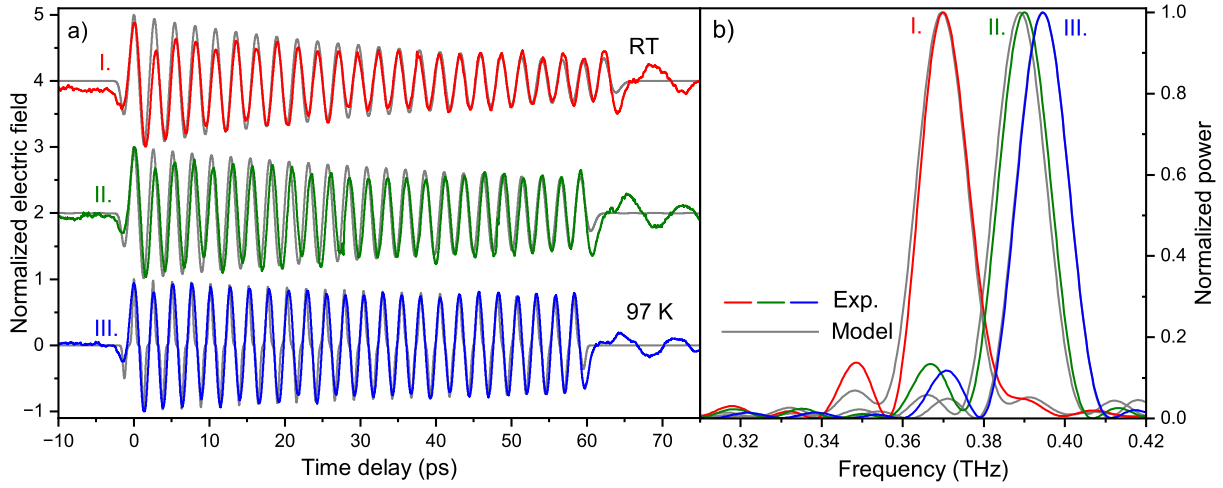

FIG. 3. Normalized THz (a) waveforms and (b) power spectra recorded and modelled for a PPLN wafer stack consisting of 48 wafers at room temperature (labelled I), and cooled to 97 K (labelled II and III). The excitation fluence was 50 mJ cm^{-2} and a positively chirped pulse duration of 1.2 ps was used for I and II, and 0.6 ps for III. The waveforms in (a) are vertically offset for clarity. See supplementary material for the unnormalized waveforms.

source term, where the total electric field at the exit surface of the PPLN stack was calculated from the sum of contributions from individual wafers, and the effects of the inter-wafer gaps were included by considering the electric field amplitude transmission coefficient of the LN-vacuum-LN gap to the contribution from each wafer (see ref. 5 for details). The model accounts for the pump pulse chirp and propagation, the linear propagation and absorption of the locally generated THz radiation in LN, and the THz amplitude and phase changes due to propagation through finite inter-wafer gaps. The key parameters of the waveform fits are the THz refractive index of LN, the THz absorption coefficient of LN (modelled using the imaginary part of the complex THz refractive index), and the inter-wafer gap distance. While the THz refractive index governs the emission frequency and the THz absorption coefficient the amplitude decay of the THz waveform, the inter-wafer gap distance impacts both, controlling the THz amplitude loss and phase shift through the inter-wafer gaps.

In Figures 3 a) and b) we obtain good agreement at RT using a THz refractive index of 5.07, a THz absorption coefficient of 3.0 cm^{-1}, and an inter-wafer gap of 7 µm. While at 97 K, we obtain good agreement using a THz refractive index of 4.955, a THz absorption coefficient of 0.3 cm^{-1}, and an inter-wafer gap of 1 µm (see supplementary material for a summary of all the

model parameters used). These values are broadly in-line with the literature values, where at 0.4 THz the refractive index and absorption coefficient for MgO-doped congruent lithium niobate at 300 K varies from 5.0 to 5.1 and 3.3 to 8.8 cm^{-1}, respectively.[14,15], and at around 100 K in the range of 0.35-0.4 THz, the refractive index and absorption coefficient vary from 4.8325 to 4.9 and 0.5 to 1.8 cm^{-1}, respectively.[15,16] While the wafer thickness also impacts the fits, in this simple model the thickness has been kept fixed at the 135 µm specified by the wafer supplier.

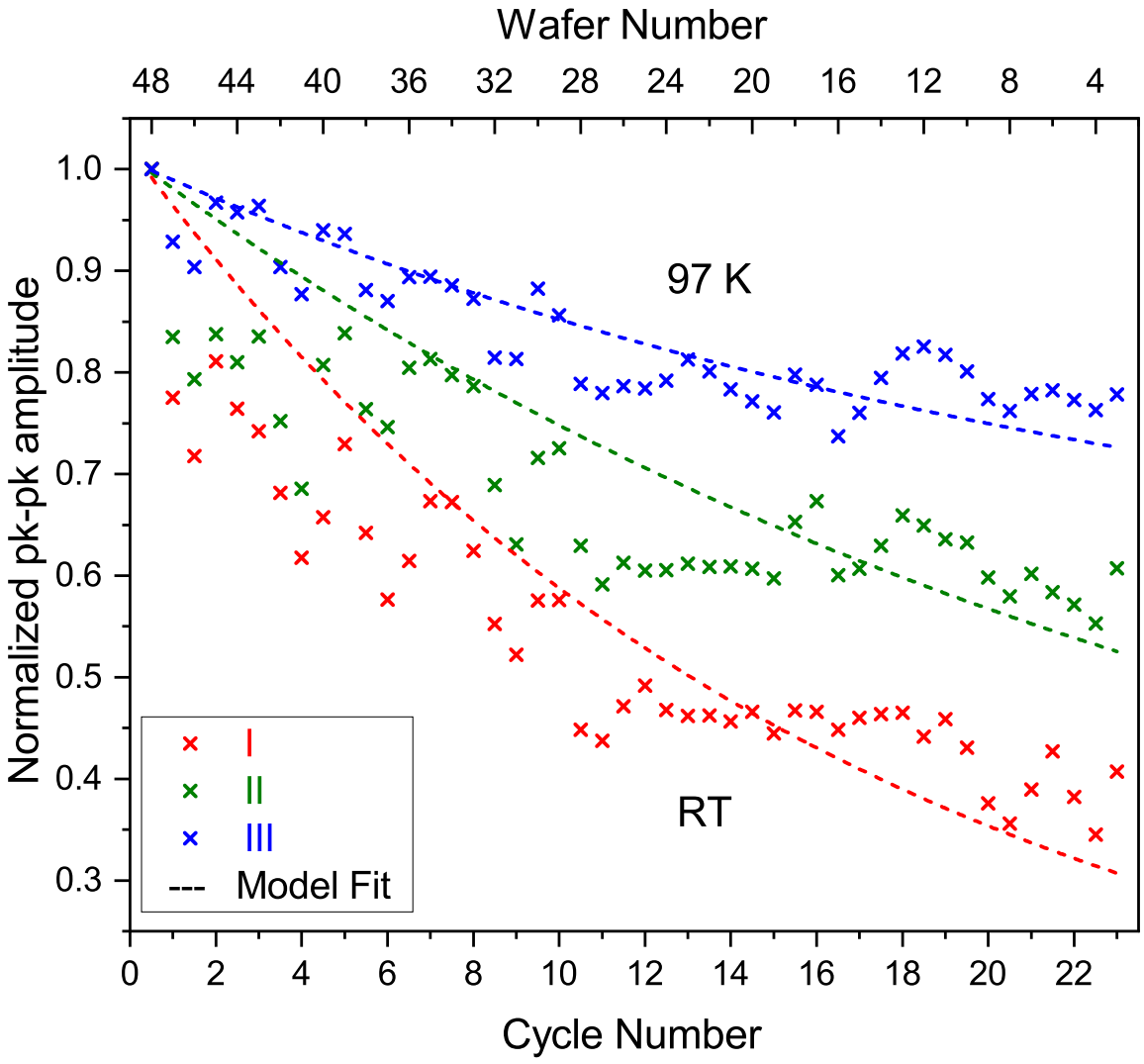

FIG. 4. Peak-to-peak amplitude of each individual waveform cycle extracted from the measured and modelled THz waveforms shown in Figure 3 for a PPLN wafer stack consisting of 48 wafers at room temperature (labelled I) and cooled to 97 K (labelled II and III).

Figure 4 shows the peak-to-peak amplitude of each individual waveform cycle from Figure 3

for the 48-wafer stack. The amplitude of the last cycle, corresponding to the THz emission from the first wafer in the stack, is clearly seen to increase as the temperature is reduced to 97 K. This is attributed to two factors, the reduced absorption of the THz radiation as it propagates through the lithium niobate wafers, and the observed reduction in the inter-wafer gap size as the stack is cooled. Using the model fit to extrapolate to greater numbers of wafers reveals that for the 97 K case, the peak-to-peak amplitude would only decay to 60% of the maximum for 80 wafers (corresponding to a waveform with 40 cycles), demonstrating the potential to reach sub-percent bandwidths.

The thickness and inter-wafer gap uniformity is evident from comparing the measured bandwidth with that calculated for a model PPLN structure. Our one-dimensional model of THz generation in a 48 wafer PPLN stack produces a power spectrum bandwidth of 14.7 GHz at 0.394 THz when the THz absorption and inter-wafer gap size are both set to zero and the wafer thickness is fixed at 135 µm (see supplementary material for the THz waveform and power spectrum of an idealised 48 wafer PPLN stack with no THz absorption or loss). This is in good agreement with the 97 K power spectrum shown in Fig. 3 b) which has a full-width at half-maximum height of 14.4 GHz at a peak frequency of 0.394 THz.

The THz energy measurements, performed using the calibrated pyroelectric detector, revealed a maximum generated THz pulse energy of 0.42 mJ exiting the UVFS window at the back of the PPLN wafer stack when the cryo-cooled 48 wafer PPLN stack was excited using 0.6 ps pump pulses with 500 mJ of energy. The THz energy was corrected for the transmission loss through the cryostat exit window, high-reflecting 1030 nm mirror, the reflectivity of the off-axis parabolic mirror, and the PTFE plate which were all positioned between the source and the detector (see supplementary material for details of the terahertz beam propagation and transmission loss). While the UVFS window aids the outcoupling, it also introduces Fresnel reflection loss. If we correct for the Fresnel reflection loss the THz energy inside the PPLN wafer stack was 0.57 mJ which corresponds to an internal conversion efficiency of 0.11%. The THz detector array was used to confirm that all the generated THz radiation was collected and focused onto the 30 mm active area of the pyroelectric detector. These measurements revealed an elliptically-shaped THz profile with major radius of 2.87 mm, minor radius of 1.89 mm at the surface of the pyroelectric detector.

The 0.42 mJ of THz pulse energy was emitted from the UVFS window at the back of the PPLN wafer stack at a repetition rate of 50 Hz equating to an average power of 21 mW. Millon *et al.*[17] provided an overview of the THz average power produced by optical rectification of materials suit-

able for pumping with 1030 nm, namely lithium niobate, gallium phosphide and a range of organic crystals. They reported average powers ranging from 9 to 34 mW depending on the source and repetition rate employed. The average THz power produced here from a hand-made PPLN wafer stack is therefore comparable to the record values produced from other materials. One particular advantage of PPLN wafer stacks however is the scalability of the source, as the output energy will simply scale with the total thickness of the stack in the absence of pump depletion and/or self-phase modulation. Given the low THz losses determined for a cryo-cooled 48 wafer stack it should be possible to increase the output energy by further increasing the number of wafers before the THz absorption and losses build to a detrimental level. Furthermore, with large-area >4"-diameter wafers of lithium niobate commercially available, these sources are fully capable of exploiting >10 J laser drivers, providing a route to narrow-bandwidth THz sources beyond the 10 mJ level. Such sources are crucial for THz-driven particle acceleration in dielectric-lined waveguides, where the aim is to match the phase velocity of a travelling THz wave to a co-propagating particle bunch.[18] The narrow bandwidth limits the deleterious THz pulse dispersion and also enables the energy contained in the THz pulse to be used efficiently by the waveguide structures due to their limited acceptance bandwidths.

In conclusion, we have demonstrated that cryogenic cooling of periodically-poled lithium niobate wafer stacks is an effective method to improve the THz emission. We have achieved an output pulse energy of 0.42 mJ, and a bandwidth of 14.4 GHz at 0.394 THz, from a PPLN wafer stack using 48 wafers cooled to 97 K. Our fitting of the experimentally measured THz waveforms with a model of THz generation has revealed that the inter-wafer gaps are sufficiently small (on the order of 1 μm at 97 K) not to have a significant detrimental effect on the emission. Our approach offers the prospect of scaling to even higher energies due to the low THz absorption and losses at cryogenic temperatures and the readily available large-area lithium niobate wafers.

The supplementary material contains the power spectra corresponding to the THz waveforms presented in Figure 2; the THz waveform and corresponding power spectrum calculated for an idealized 48 wafer PPLN stack with no THz loss; the results of a terahertz beam propagation calculation and the transmission of the THz beam path; a photograph of the edge of the PPLN wafer stack; and the unnormalized THz waveforms and the model parameters used in Figure 3.

This work was supported by the United Kingdom Science and Technology Facilities Council

[Grant No. ST/V001612/1], and the Hungarian National Research, Development and Innovation Office [Grant No. ANN 139483]. The ELI-ALPS project (GINOP-2.3.6-15-2015-00001) is supported by the European Union and co-financed by the European Regional Development Fund.

DATA AVAILABILITY

The data associated with the paper are openly available from the Zenodo data repository at: http://dx.doi.org/xx.xxxxx/xxxxxxxxxxxx.

REFERENCES

[1]K. Uchida, H. Hirori, T. Aoki, C. Wolpert, T. Tamaya, K. Tanaka, T. Mochizuki, C. Kim, M. Yoshita, H. Akiyama, L. N. Pfeiffer, and K. W. West, Appl. Phys. Lett. **107**, 221106 (2015).

[2]T. Lin, R. Xu, X. Chen, Y. Guan, M. Yao, J. Zhang, X. Li, and H. Zhu, ACS Photonics, **11**, 33 (2024).

[3]M. T. Hibberd, A. L. Healy, D. S. Lake, V. Georgiadis, E. J. H. Smith, O. J. Finlay, T. H. Pacey, J. K. Jones, Y. Saveliev, D. A. Walsh, E. W. Snedden, R. B. Appleby, G. Burt, D. M. Graham, and S. P. Jamison, Nat. Photonics **14**, 755 (2020).

[4]F. Lemery, T. Vinatier, F. Mayet, R. Assmann, E. Baynard, J. Demailly, U. Dorda, B. Lucas, A.-K. Pandey, and M. Pittman, Commun. Phys. **3**, 150 (2020).

[5]C. D. W. Mosley, D. S. Lake, D. M. Graham, S. P. Jamison, R. B. Appleby, G. Burt, and M. T. Hibberd, Opt. Express **31**, 4041 (2023).

[6]L. Pálfalvi, J. Hebling, J. Kuhl, A. Péter, and K. Polgár, J. Appl. Phys. **97**, 123505 (2005).

[7]J.-I. Shikata, M. Sato, T. Taniuchi, H. Ito, and K. Kawase, Opt. Lett. **24**, 202 (1999).

[8]C. Vicario, B. Monoszlai, Cs. Lombosi, A. Mareczko, A. Courjaud, J. A. Fülöp, and C. P. Hauri, Opt. Lett. **38**, 5373-5376 (2013).

[9]S.-W. Huang, E. Granados, W. R. Huang, K.-H. Hong, L. E. Zapata, and F. X. Kärtner, Opt. Lett. **38**, 796 (2013).

[10]Y.-S. Lee, T. Meade, M. DeCamp, T. B. Norris, and A. Galvanauskas, Appl. Phys. Lett. **77**, 1244 (2000).

[11]S. Carbajo, J. Schulte, X. Wu, K. Ravi, D. N. Schimpf, and F. X. Kärtner, Opt. Lett. **40**, 5762 (2015).

[12]S. W. Jolly, N. H. Matlis, F. Ahr, V. Leroux, T. Eichner, A.-L. Calendron, H. Ishizuki, T. Taira, F. X. Kärtner, and A. R. Maier, Nat. Commun. **10**, 2591 (2019).

[13]THz Pump Lasers – ELI User Portal, https://up.eli-laser.eu/laser/thz-pump-lasers-819232877.

[14]M. Unferdorben, Z. Szaller, I. Hajdara, J. Hebling, and L. Palfalvi, J. Infrared Millim. Terahertz Waves **36**, 1203 (2015).

[15]X. Wu, C. Zhou, W. R. Huang, F. Ahr, and F. X. Kärtner, Opt. Express **23**, 29729 (2015).

[16]N. H. Matlis, Z. Zhang, U. Demirbas, C. Rentschler, K. Ravi, M. Youssef, G. Cirmi, M. Pergament, M. Edelmann, S. M. Mohamadi, S. Reuter, and F. X. Kärtner, Opt. Express **31**, 44424 (2023).

[17]C. Millon, S. Houver, and C. J. Saraceno, Opt. Express **31**, 7922 (2023).

[18]L. J. R. Nix, J. T. Bradbury, C. T. Shaw, M. T. Hibberd, D. M. Graham, R. B. Appleby, G. Burt, R. Letizia, and S. P. Jamison, Phys. Rev. Accel. Beams **27**, 041302 (2024).